Published in final edited form as:
Stem Cells. 2008 February ; 26(2): 474–484. doi:10.1634/stemcells.2007-0303.

Activin Alters the Kinetics of Endoderm Induction in Embryonic Stem Cells Cultured on Collagen Gels

Natesh Parashurama[1,2], **Yaakov Nahmias**[1], **Cheul H. Cho**[1], **Daan van Poll**[1], **Arno W. Tilles**[1], **François Berthiaume**[1], and **Martin L. Yarmush**[1,2]

[1] Center for Engineering in Medicine and Surgical Services, Massachusetts General Hospital, Harvard Medical School, 51 Blossom St, Boston, MA 02114, U.S.A

[2] Rutgers, The State University of New Jersey, Department of Chemical and Biochemical Engineering, Rutgers University, The State University of New Jersey, 98 Brett Road, Piscataway, NJ 08854, U.S.A

Abstract

Embryonic stem cell-derived endoderm is critical for the development of cellular therapies for the treatment of disease such as diabetes, liver cirrhosis, or pulmonary emphysema. Here, we describe a novel approach to induce endoderm from mouse embryonic stem cells (mES) using fibronectin-coated collagen gels. This technique results in a homogenous endoderm-like cell population, demonstrating endoderm-specific gene and protein expression, which remains committed following in vivo transplantation. In this system, activin, normally an endoderm inducer caused an 80% decrease in the Foxa2 positive endoderm fraction, while follistatin increased the Foxa2 positive endoderm fraction to 78%. Our work suggests that activin delays the induction of endoderm through it transient precursors, the epiblast and mesendoderm. Long term differentiation, displays a two-fold reduction in hepatic gene expression and three-fold reduction in hepatic protein expression of activin-treated cells compared to follistatin-treated cells. Moreover, subcutaneous transplantation of activin-treated cells in a syngeneic mouse generated a heterogeneous teratoma-like mass, suggesting these were a more primitive population. In contrast, follistatin-treated cells resulted in an encapsulated epithelial-like mass, suggesting these cells remained committed to the endoderm lineage. In conclusion, we demonstrate a novel technique to induce the direct differentiation of endoderm from mES cells without cell sorting. In addition, our work suggests a new role for activin in induction of the precursors to endoderm, and a new endoderm-enrichment technique using follistatin.

Keywords

Activin; Endoderm; Collagen Gel; Embryonic Stem Cells (Mouse); Follistatin; Epiblast

Introduction

Embryonic stem cells-derived endoderm progenitors offer a remarkable potential for the treatment of major diseases effecting the pancreas, liver, lungs, bladder, and prostate [1,2]. Endoderm progenitors would also be useful for the study of congenital diseases [3], gene discovery, toxicology screening, and drug development [4]. Current knowledge regarding the development of the definitive endoderm, one of three major germ layers, is derived from in vivo fate mapping [5–7], mouse genetics [8], in vitro tissue explants, [9] and recent microarray

Corresponding Author: Martin L. Yarmush, ireis@sbi.org, 617-371-4882, 617-726-3474, Fax # 617-573-9471, The Center for Engineering in Medicine, 114 16th Street, Room 1402, Charlestown, MA 02129-4404.

analysis of prospective endoderm [10]. These studies indicate that the endoderm is derived from the inner cell mass through the differentiation of the transient epiblast and mesendoderm (anterior primitive streak) populations [11]. Each of these populations express unique markers or transcription factors. For example, the epiblast expresses Oct4 and Fgf5, mesendoderm expresses Brachyury and Foxa2, [12] and endoderm expresses Foxa2 and Sox 17 [13] [14]. The ability to identify and control these transient precursor populations is a major goal of the field [15,16]. While endoderm induction has not been studied extensively, several recent studies have focused on ideal culture conditions for hepatocyte induction, an important product of endoderm differentiation. [17–21]

Endoderm induction has been shown to be controlled by soluble factors such as activin-nodal-TGFβ, BMP, and Wnt [22–27]. Recent studies demonstrated that definitive endoderm can be derived from a mesendoderm precursor, using serum-free medium, activin, and serial cell sorting [15,28]. Activin, which binds to the same receptor as nodal [29] has been shown to generate different tissues as a function of concentration in both Xenopus and mouse embryonic stem (mES) cell studies, and has therefore been classified as a potent developmental morphogen [30]. However, recent studies suggest that while activin enhanced endoderm in embryiod body (EB) cultures, it failed to do so in monolayer culture [10]. Furthermore, in human ES cells, activin-nodal signaling was shown to inhibit ES cell differentiation, rather than induce endoderm. [31–34] A similar mechanism was shown to inhibit the differentiation of inner cell mass cells in ex vivo mouse blastocyst cultures [32] suggesting a complex role of activin-nodal signaling in ES cell differentiation. The role that follistatin plays in vitro studies is unclear. [35] However, recent studies suggest that follistatin has an important role during liver regeneration [36] and pancreas differentiation [37].

Studies thus far have relied on multiple cell sorting, complex serum-free formulations, and multiple growth factors for the differentiation of endoderm. Here, we describe a simple cell culture system which induces the differentiation of mES cells toward endoderm in the presence of serum without cell sorting, growth factors, or hormones. The endoderm-like cell population was positive for endoderm specific markers Foxa2 and Sox17 and negative for major mesodermal and ectodermal markers by day 10 of culture. Surprisingly, activin caused a dose-dependent decrease in the expression endoderm markers, while inducing the expression epiblast and mesendoderm markers, such as Brachyury and Fgf5. On the other hand, the activin-inhibitor follistatin increased the Foxa2 positive endoderm fraction to 78.4%, without altering the expression kinetics. Long term gene and protein expression studies indicated that activin-treated cells had reduced hepatic differentiation potential compared to follistatin and controls. In vivo differentiation of activin-treated cells in a syngeneic mouse model generated a heterogeneous, teratoma-like mass, suggesting a primitive population, while follistatin-treated cells generated an encapsulated epithelial-like mass, similar to control. In conclusion, these studies demonstrate a novel technique to induce an endodermal cell population in vitro and suggest an intriguing role of activin in endoderm development.

Methods

Reagents

Fetal Bovine Serum (FBS), Dulbecco's modified Eagle medium (DMEM), penicillin, streptomycin, knockout serum, knockout DMEM, bovine gelatin, and dispase were obtained from Invitrogen Life Technologies (Carlsbad, CA). Human Fibronectin was purchased from BD Biosciences (San Jose, CA, USA). Hydrocortisone was obtained from Pharmacia (Kalamazoo, MI). Glucagon and Insulin were purchased from Eli-Lilly (Indianapolis, IN). Oncostatin M, Human Bone Morphogenic Protein-2 (BMP2), Hepatocyte Growth Factor (HGF), Human Activin, Mouse Follistatin, were purchased from R&D Systems (Minneapolis, MN). ESGRO (Recombinant Leukemia Inhibitory Growth Factor) was purchased Chemicon

(Temecula, CA). Immunofluorescence grade paraformaldehyde was purchased from Electron Microscope Sciences (Hatfield, PA). Rabbit anti-mouse Foxa2 antibody was purchased from R&D Systems (Minneapolis, MN). Goat anti-mouse Sox17 was purchased from Santa Cruz (Santa Cruz, CA). Goat anti-mouse Albumin was purchased from ICN Pharmaceuticals (Aurora, OH). For immunofluorescence studies, normal donkey serum and secondary F(ab)2 antibody fragments, ML grade, were obtained from Jackson Immunoresearch (Bar Harbor, ME). Unless otherwise noted, all other chemicals, growth factors, and solutions were purchased from Sigma-Aldrich Chemicals.

Embryonic stem cell culture

Undifferentiated mouse D3-ES cells (ATCC) were cultured on 0.2% gelatin-coated tissue culture T75 flasks, at low dilutions of 1:50, such that small colonies were maintained. Medium was changed daily. Experiments were carried out with cells at passage 30. Undifferentiated mES cells were cultured in Knockout DMEM supplemented with 15% Knockout serum, L-Glutamine (4 mM), Penicillin(100 U/ml), Streptomycin (100 U/ml), Gentamicin (10 mg/ml), ESGRO (1,000 U/ml), and 2-Mercaptoethanol (0.1 mM). Proliferating ES cell cultures were maintained in a 5% CO_2 humidified incubator at 37°C.

Fibroblast cell culture

NIH 3T3 mouse fibroblasts (ATCC) were cultured at 1:10 dilution on tissue culture-treated T75 flasks in high glucose DMEM containing 10% FBS, Penicillin (100 U/ml), Streptomycin (10 mg/ml), Gentamicin (1,000 U/ml) and medium was changed every 2 days.

Fibronectin-coated collagen gels

Type I collagen stock solution was prepared from rat tail tendon as described by Dunn *et al* [38]. Collagen gelling solution was prepared by mixing nine parts of collagen stock (1.25 mg/ml) with one part of 10 × DMEM on ice. The collagen gelling solution was then added at a volume of 250 μl/well (66 μl/cm^2), spread evenly on the dish and incubated at 37°C for 30 min for gel formation. Fibronectin dissolved in PBS was then added on top of the gel, at a concentration at 3.8 μg/well (1 μg/cm^2) and the tissue culture plates were incubated for 1h at 37°C to insure ensure fibronectin adsorption on collagen gel.

Mouse embryonic stem (mES) cell differentiation

Mouse embryonic stem (mES) cells were directly seeded at a density of 2×10^4 cells/well (5.2×10^3 cells/cm^2) onto fibronectin-coated collagen gels. Basal differentiation medium consisted of high glucose DMEM supplemented with 10% Fetal Bovine Serum, Glutamine (100 U/ml), Penicillin (100 U/ml), Streptomycin (100 U/ml), Gentamycin (10 mg/ml). For growth factor studies, the medium was augmented with activin (20 or 50 ng/ml) or follistatin (100 ng/ml). Medium was changed every 2 days of culture. Differentiating ES cell cultures were maintained in a 10% CO_2-humidified incubator at 37°C.

Embryoid Body (EB) cultures were formed by culturing mES cells using the hanging drop method. ES cells were resuspended in differentiation medium and spotted as 30 μl drops on an inverted lid of a 100 mm dish at a concentration of 30,000 cells/ml. Dishes were incubated at 37°C for 48h in PBS. EB's were recovered and matured in suspension for 48h and then transferred to a 12 well plate.

Late stage in vitro ES cell maturation

Following 10 days of culture, the endoderm-like cells were harvested from gel culture using dispase digestion (1 mg/ml), and filtered using a sterilized 200 μm nylon mesh. Viability was greater than 92%. The harvested endoderm-like cells were then seeded onto fibronectin-coated

collagen gels at a concentration of 5×10^4 cells/well (1.3×10^4 cells/cm^2) in C+H medium, consisting of high glucose DMEM supplemented with 10% heat-inactivated fetal bovine serum, penicillin/streptomycin (100 U/ml), hydrocortisone (7.5 g/ml), epidermal growth factor (20 ng/ml), glucagon (14 ng/ml), and insulin (0.5 U/ml). C+H medium was augmented with Bone Morphogenic Protein-2 (BMP2) (10 ng/ml), Hepatocyte Growth Factor (HGF) (20 ng/ml) and Oncostatin M (OSM) (20 ng/ml).

Late stage in vivo syngeneic mouse transplantation

Female 129 mice, (Charles River Laboratories, Boston, MA), syngeneic to D3 ES cells, and weighing between 25 and 35 g were used for this study. The animals were cared for in accordance with the guidelines set forth by the Committee on Laboratory Resources, National Institutes of Health, and Subcommittee on Research Animal Care and Laboratory Animal Resources of Massachusetts General Hospital. Animals had free access to food and water.

ES cells were recovered using dispase digestion from either EB plated culture, standard collagen culture, activin-treated, or follistatin-treated cultures and filtered using a sterilized 200 μm nylon mesh. For support of cellular function, 3×10^6 mES cells were mixed with 3×10^4 mouse NIH 3T3 fibroblasts. Mice were anesthetized with intraperitoneal injections of pentobarbitol (70mg/kg). After shaving and cleaning the site of injection with antiseptic solution, cells were injected subcutaneously such that a subcutaneous wheal could be identified in the paraspinal region between the 6th and 8th rib using a 28-guage needle. Permanent stitches were placed to mark the injection site. Two weeks after injection, animals were killed by cervical dislocation and the transplantation site was excised and fixed in formalin. Abdominal and thoracic cavities were inspected for tumor formation.

H&E staining

Tissue samples were fixed in buffered formalin (1:10) and placed in tissue cassettes, dehydrated, embedded in paraffin, and sectioned at 4μm. Standard H&E (Hematoxylin and Eosin) staining was performed. Slides were examined using a Nikon Eclipse 800 upright compound microscope and analyzed using Advanced Spot 2 software (Molecular Dynamics).

Reverse Transcriptase Polymerase Chain Reaction (RT-PCR)

For each experimental condition, cell lysates were generated using Gaunidinium Isothiocyanate-based solution (Clonetech) and stored at −80°C for later use. RNA isolation was conducted using the manufacturer's instructions for the Nucleospin II RNA Kit (Clonetech). RNA gels were run using 2% Agarose (RNAase free) to ensure that RNA was intact prior to RT-PCR. One-step gene-specific RT-PCR (Qiagen) was performed for gene expression analysis and resolved on a 2% agarose gel. Each reaction represents 10 micrograms of total RNA per condition. Cycle number was 30 for all genes unless otherwise specified. Cycling conditions were 55°C, 30 sec, 94°C, 30 sec, and 72°C 30 sec, with a ten minute extension at 72°C. Thermal cycling was done using the Mastercycler Epigradient X (Eppendorf) with 96 well plates Gels were imaged using fluorescent gel scanner, the Fluor-S Multi-Imager (BioRad) and captured using Multi-analyst software. Primers were as follows:

B-Actin (F) 5′-GAGGGAAATCGTGCGTGA-3′; *B-Actin* (R) 5′ CCAAGAAGGAAGGCTGGAA-3′;

Oct4 (F) 5′-GGAAAGCCGACAACAATGA-3′; *Oct4* (R) 5′-CAAGCTGATTGGCGAATGT-3′;

Fgf5 (F) 5′-GTTCAAGCAGTCCGAGCAA-3′; *Fgf5* (R) 5′-TAGGCACAGCAGAGGGATG-3′;

Otx2(F); 5′-GGAAGGGAGGGAAGGTCAT-3′; *Otx2*(F) 5′-CAG-TCGCACAATCCACACA-3′;

Brachyury (F) 5′-AAGAACGGCAGGAGGATGT-3′;

Brachyury (R) 5′ GCGAGTCTGGGTGGATGTA-3′;

Goosecoid (F) 5′ GCACCGCACCATCTTCA-3′; *Goosecoid* (R) 5′-GTTCCACTTCTCGGCGTTT-3′;

Otx2 (F) 5′-GGAAGGGAGGGAAGGTCAT-3′; *Otx2* (R) 5′-CAGTCGCACAATCCACACA-3′;

Lhx1 (F) 5′-CTGACACGCACACAACCTG-3′; *Lhx1* (R) 5′-GCGGCTCTTCTGCTCAAA-3′;

Hnf1β (F) 5′-GCCAGTCGGTTTTACAGCA-3′; *Hnf1β* (R) 5′-TGGGCTTGGGAGGTGTT-3′;

Foxa1 (F) 5′-GCCGCCTTACTCCTACATCTC-3′; *Foxa1* (R) 5′-TGCCACCTTGACGAAACA-3′

Foxa2 (F) 5′-ACACGCCAAACCTCCCTAC-3′; *Foxa2* (R) 5′-GGGCACCTTGAGAAAGCA-3′;

Sox17 (F) 5′-ATCCAACCAGCCCACTGA-3′; *Sox 17* (R) 5′-TCGGCAACCGTCAAATG-3′;

Alb1 (F) 5′-CCCTGTTGCTGAGACTTGC-3′; *Alb1* (R) 5′-TGAGGTGCTTTCTGGGTGT-3′;

CK8 (F) 5′-AAACCCGAGATGGGAAGC-3′; *CK8* (R) 5′-GCCAGAGGATTAGGGCTG-3′

CK18 (F) 5′-CAAGGTGAAGAGCCTGGAAA; *CK18* (R) 5′-AAGTCATCGGCGGCAAG-3′

Pdx1(F) 5′-ACCTCCTCGTGCCCCTAAT-3′; *Pdx(R)* 5′-CCTGCTCCTCTCTCCATCT-3′;

Ins1 (F) 5′-CAGCAAGCAGGTCATTGTTT-3′; *Ins1(R)* 5′-AACGCCAAGGTCTGAAGG-3′;

IFABP (F) 5′-TGACAATCACACAGGATGGA-3′; *IFABP* (R) 5′-TCTCGGACAGCAATCAGC-3′;

Gata1 (F) 5′-CACCATCAGGTTCCACAGG-3′; *Gata1* (R) 5′-TTGAGGCAGGGTAGAGTGC-3′;

Foxf1 (F) 5′-CGTGTGTGATGTGAGGTGAG-3′; *Foxf1* (R) 5′-CTCCGTGGCTGGTTTCA-3′;

Runx2 (F) 5′-TTCCAGACCAGCAGCACTC-3′; *Runx2* (R) 5′-GCCGCCAAACAGACTCAT-3′;

Lefty2 (F) 5′-CCGTTGTTCCCATTTCTC-3′; *Lefty2* (R) 5′-GGACTGTGCTGTGCTGTGTC-3′

Paraxis(F) 5′-TCCAGAAGCCCAAACCAC-3′

Paraxis(R) 5′-TGCTCACATACTACATTCACACAGA-3′

Ascl1 (F) 5′-TGTGACGCTCTTGCTCCA-3′; *Ascl1* (R) 5′-GCTGCCCTCGGTCTATTTC-3′;

Pax6 (F) 5′-TGCCCTTCCATCTTTGCT-3′; *Pax6* (R) 5′-CCATCTTGCGTGGGTTG-3′;

Neurog2 (F) 5′-TGAGCCAGTCACAAAGAAGGT-3′;(R) 5′ GCAGGCAGTTCGTGTGAA-3′

Quantitative Real-Time RT-PCR

Reverse transcription and qPCR was performed using the Superscript III Two-Step qRT-PCR kit (In Vitrogen, Catalog No 11735-032). The RT reaction was run using primer containing a mixture of random-hexamers and dT primers, 500ng of total RNA template, and master mix containing a bioengineered MMLV-RT enzyme, nucleotides, and other components. The reaction mix was incubated at 25°C for 10 minutes, and 42°C for 50 minutes, followed by termination at 85°C for 5 min and RNAaseH incubation at 37°C for 20 minutes. Real-time quantitative PCR was performed using the Stratagene MX5000P QPCR machine. Triplicates of 10 μL reactions containing 2 μL of primer mixture (0.2 μM), 10 ng of cDNA template, Rox dye, and SYBR Green master mix containing the Platinum Taq Polymerase were used for all reactions. The cycling temperatures were 94°C for 30s, 57°C for 30s, 72°C for 30s.

Relative Quantitation of Real-Time PCR data

Real time data was analyzed using the Stratagene MX-Pro QPCR software using settings with an amplification-based threshold and adaptive baseline. Melting curves for each reaction were obtained and any reactions without a unique PCR product were not analyzed. Threshold cycle (CT) were determined and used to quantify gene expression using the $2^{-\Delta\Delta Ct}$ method [39]. Gene expression was measured relative to a normalizer, β-Actin, and calibrated using the day 0 condition for the genes of interest. This data, which was then expressed as relative difference of gene expression on day 24 compared to day 0, was normalized to the untreated condition, termed control. Thus the activin-treated and the follistatin treated conditions were normalized to the control condition.

Immunofluorescence

Samples were washed three times with PBS, and fixed in 4% EM-grade paraformaldehyde for 10 min at room temperature. Samples were then washed with PBS and were permeabilized for 15 min with 0.1% Triton X-100, blocked for 30 min with 1% bovine serum albumin, 5% donkey serum at room temperature followed by staining with primary antibodies at overnight at 4°C. The dilutions of primary antibodies used were Foxa2 (1:100), Sox 17 (1:100) and albumin (1:500). After additional washes with PBS, samples were stained with fluorescently tagged secondary antibodies at a dilution of 1:500, for 45 min at room temperature and washed three times with PBS. Cells were then imaged using phase contrast and fluorescent microscopy (Ziess) and captured using AxioVert software.

Flow cytometry

Samples were washed three times with cold PBS, kept on ice, and fixed in 1% EM-grade paraformaldehyde for 15 min at 4° C. Samples were then washed with ice cold PBS and were permeabilized for 15 min with 0.1% Triton X-100 while cells were vortexing, and then washed twice with cold PBS. Cells were blocked for 30 min with 1% bovine serum albumin, 5% donkey serum at room temperature for 30 min. Primary antibodies diluted in blocking buffer (above) were then added for 20 min at room temperature, at the same dilution as for immunoflourescence. After additional washes with ice cold PBS, samples were stained with fluorescently tagged secondary antibodies, at the same dilution as immunoflourescence, for 45

min at room temperature, and then washed twice again. Flow cytometry was conducted on a Coulter Epics Altra Flow Cytometer (Beckman Coulter) and raw data were captured using Expo 32 Multicomponent software.

RESULTS

Culture of ES cells on collagen gels selectively induces endoderm gene and protein expression

The culture of epithelial cells on collagen gels was previously shown to promote epithelial polarity and function [40]. In order to determine the ability of the collagen gel culture to induce an endodermal phenotype we cultured mouse ES cells at 5,000 cells/cm^2 seeding density on fibronectin-coated collagen gels, in the presence of 10% serum. By day 10, the cells acquired a characteristic epithelial morphologically with bright cell borders reminiscent of endoderm-like cells [41–43](Figure 1a). In contrast, mouse ES cells cultured on tissue culture plastic coated with a thin layer of collagen and fibronectin formed a morphologically mixed population with numerous spindle-like cells in addition to the epithelial population. Embryoid body culture (EB) outgrowths demonstrate a clear heterogeneous morphology by day 10 (Figure 1a). To clarify serum effects in our system, we compared our results with the current paradigm of serum-free as well as low serum conditions. Mouse ES cells were seeded on fibronectin-coated collagen gels in serum free media previously used by Kubo et al. 2004. The cells failed to adhere or proliferate suggesting a critical component was missing in the serum-free formulation (Figure 1a, Supplemental). As a result we were unable to obtain sufficient sample for analysis of gene expression. Furthermore, gene expression studies on mES cells cultured in low-serum conditions (1% and 5%) demonstrated a increased Fgf5 expression, suggesting a more primitive phenotype (Figure 1b, Supplemental).

To determine if the observed morphologies correlated with particular genetic phenotypes, we studied the day 10 populations using RT-PCR. Day 10 mouse embryonic RNA was used for a positive control for all primers. We detected endodermal (Foxa2 and Sox17) but not mesodermal (Foxf1, Runx2, GATA1) [44–46] genes in all three conditions (Figure 1b). As expected, only the EB condition expressed transcripts for the ectodermal gene Ascl1 [47]. To determine if the collagen gel-cultured cells with epithelial-like morphology expressed endoderm-specific markers, we performed immunofluorescence staining for the major endoderm transcription factors Foxa2 and Sox17. We found that nearly all cells with epithelial-like morphology expressed both Foxa2 and Sox 17 (Figure 1c). To determine the relative fraction of these endoderm-like cells, we used flow cytometry, demonstrating that approximately 53% of the cells were positive for Foxa2 by day 10 of culture (Figure 1d).

Activin decreases endoderm and increases epiblast-specific gene expression

Activin/Nodal is a member of the TGFβ superfamily, which has been previously shown to be critical in regulating endoderm formation in vitro [28,43] and in vivo [48]. To test whether endoderm induction in gel cultures responded to stimulation of the activin/nodal axis, we added activin or follistatin (a soluble inhibitor of activin) to the serum-containing culture medium from day 0 to day 10. The addition of 50 ng/ml activin induced the appearance of elongated, spindle-like cells, by day 6 of culture (Figure 2a). In contrast, follistatin-treated cells appeared to have epithelial like morphology similar to control (Figure 2a).

We then analyzed these day 10 populations by RT-PCR for epiblast (Oct4, Fgf5) [49], endoderm (Foxa2, Sox 17), mesoderm (GATA1, Runx2, Foxf1) [44,45], early mesodermal patterning (Paraxis, Lefty2) [50,51], and neurectoderm (Pax6, Ascl1(Mash1), Ngn2) markers [47,52] (Figure 2b). Surprisingly, the addition of activin (20 ng/ml and 50 ng/ml) decreased endoderm gene expression in a dose dependent manner (Figure 2b), while the addition of

follistatin (100 ng/ml) did not. Interestingly, this decrease in Foxa2 and Sox17 expression in the activin condition correlated with an increase in expression of the primitive epiblast markers Oct4 and Fgf5. As expected, follistatin had the opposite effect, decreasing Fgf5 expression compared to controls. Neurectodermal and mesodermal markers were absent in all conditions (data not shown.) Mesodermal patterning markers, which are activated prior to mesodermal specification in vivo, showed a dose-dependent increase in gene expression with activin, while follistatin induced a downregulation of these genes (Figure 2b).

Immunoflourescence staining for Foxa2 and Sox17 indicated that the activin-treated spindle-like cells did not express Foxa2 or Sox 17 on the protein level, while follistatin-treated epithelial cells had strong Foxa2 and Sox 17 expression (Figures 2c, 2d). To quantify the percentage of endodermal cells, we performed flow cytometry for Foxa2 on day 10 of culture. Activin-treated cells (50 ng/ml) had approximately 10% Foxa2 positive cells while follistatin-treated cells were approximately 78% Foxa2 positive cells (Figure 2e). Thus, activin decreased the endodermal fraction by 80% while follistatin caused a 47% increase. These results suggest that activin might delay endoderm induction by maintaining upregulation of early genes for epiblast or mesodermal patterning.

Activin alters the gene expression kinetics of epiblast, mesendoderm, and endoderm

Previous studies have indicated that the and Oct4 positive, Fgf5 positive epiblast population is a transient population which emerges on embryonic day 2 (E2) and is down-regulated by E5 as the cells differentiate into the three major germ layers (ectoderm, mesoderm, endoderm) [53]. Our previous results (Fig 2b) demonstrated that while activin downregulated endoderm genes by day 10 of culture, it also upregulated the early epiblast gene Fgf5. To determine if the kinetics of the epiblast precursor population is altered in the presence of activin, we analyzed epiblast (Oct4, Fgf5, Otx2) [54] mesendoderm (Brachyury, Goosecoid, and Lim1) [28,43] and endoderm (Foxa2, Foxa1, Sox17, HNF1β) specific gene expression at days 4, 6, and 10 of culture, on collagen gel in the presence of activin (20 and 50 ng/ml) or follistatin (100 ng/ml). Oct4 is a specific marker for the inner cell mass as well as the epiblast, Fgf5 is specific for epiblast, while Otx2 is expressed in epiblast in addition to other tissues during development [55]. While control cells have a decreasing expression of Oct4, Fgf5 and Otx2, activin-treated cells appear to have a constant (20 ng/ml) or increasing (50 ng/ml) expression of the same genes, suggesting an earlier phenotype or delayed differentiation. Similarly to the changes in epiblast expression, markers of mesendoderm differentiation (Brachyury, Goosecoid and Lim1) [28,43] were downregulated by day 10 of culture in control and follistatin-treated condition following transient expression, but remained upregulated by day 10 of culture in activin-treated cells.

The expression kinetics of the endoderm-specific transcription factors Foxa2 and Sox17 appear to be similar in all conditions, increasing over time (Figure 3). However, activin-treated cells appear to express lower levels of the genes in a dose-dependent manner while follistatin-treated cells express relatively higher levels of endodermal expression. Furthermore, increasing the dose of activin from 20 ng/ml to 50 ng/ml delayed the expression of Foxa1, and diminished expression of HNF1β by day 10 of culture. Taken together, the data suggests that increasing activin concentration may shift the kinetics of epiblast, and mesendoderm differentiation, from a rapid downregulation to a persistent expression of the same markers under our culture conditions.

Long term endoderm differentiation following activin stimulation

The patterning of endoderm into its downstream lineages, such as liver, pancreas, and gut, is subject to complex mechanisms in vivo and as a result, is poorly understood [1]. To test the differentiation potential of activin and follistatin-treated cells, we reseeded day 10 cells in

hepatic differentiation medium containing BMP2, HGF and Oncostatin [56] but without follistatin or activin. Analysis of cell morphology on days 14, 18, and 22 demonstrated that the cells originating from all three early-differentiation conditions, control, activin (50 ng/ml) and follistatin (100 ng/ml) acquired an epithelial morphology (Figure 4a). However, activin-treated cells initially formed small clusters reminiscent of EBs formed by primitive mES cells (Figure 4a).

To determine the extent of endoderm induction and patterning, we analyzed gene expression for endoderm patterning markers following 14 days of late-stage differentiation (day 24 of total culture) by RT-PCR. We tested Foxa2 and Sox17, as well the foregut marker alpha fetoprotein (AFP), Albumin, Pdx1, and Insulin [57], the midgut marker Cdx2 [58] and the hindgut maker Intestinal Fatty Acid Binding Protein, (IFABP) [58]. Day 10 mouse embryonic RNA was used for a positive control for all primers. Expression of Foxa2, Sox17 and AFP was similar in all three conditions (Figure 4b). However, the expression foregut marker albumin as well as the hindgut marker IFABP were inhibited by activin but stimulated by follistatin (Figure 4b), suggesting that activin might delay hepatic differentiation. To quantify these phenomenon, we performed qRT-PCR on two genes known to be markers for hepatic differentiation, cytokeratin 8 (CK8) and cytokeratin 18(CK18) (Figure 4c). When compared to control, activin-treated cells displayed decreased relative expression of CK 8 (0.705 ± 0.106) and CK18 (0.79± 0.14). On the other hand follistatin-treated cells, displayed increased relative expression of both CK8 (1.43±0.32) and CK 18 (1.71±0.84). The ratio of follistatin to activin expression at day 24, was calculated to be 2.02 ± 0.153 for CK8 and 2.09 ± 0.68 for CK18. We extended the analysis of day 24 samples to examine concomitant differences in protein expression. Immunoflourescence staining for intracellular albumin on day 24 showed higher expression in control and follistatin-treated cells than in activin-treated cells (Figure 4d). To quantify the changes in albumin, we performed flow cytometric analysis of control, activin-treated, and follistatin-treated cells (Figure 4e). In control and follistatin conditions, 21.8% and 19.3% of cells were positive for albumin, whereas only 5.9% of the activin-treated cells were albumin positive. The mean intensity values of the albumin-positive population (Table 1) were 25.1% for control, 30.2% for follistatin, and 15.8 % for activin. Taken together with the endpoint PCR data, this data strongly suggests that hepatic differentiation was diminished following activin-treatment.

Long term in vivo differentiation of activin and follistatin-treated cells in a syngeneic mouse transplant model

The in vitro differentiation data on days 10 and 24 of culture suggests that while follistatin induces an endoderm-specific differentiation, activin delays differentiation through the induction of primitive lineages. To assess the differences in potency and commitment between these conditions, we transplanted day 10 cultured ES cells subcutaneously in a syngeneic mouse model. The four conditions transplanted were embryiod body (EB), control (no treatment), activin (50 ng/ml), and follistatin (100 ng/ml). Each cell population was mixed with a low ratio of NIH 3T3 fibroblasts (1:100), for mesenchymal support upon transplantation [59]. All implants gave rise to an observable mass (Figure 5a) by day 14 of transplant (day 24 total culture). The cell mass was significantly larger in the case of activin-treated cells (Figure 5b).

The excised tissue was analyzed by histological examination and was reviewed by a blinded pathologist. When cells were recovered from an embryoid body (EB) and implanted, they generated a teratoma-like cell mass with extensive extracellular matrix suggesting immature bone or cartilage, evidence of skin, glandular tube-like structures and immature cells (Figure 5f). On the other hand, the endoderm-like cell population differentiated on fibronectin-coated collagen (control) generated an encapsulated tissue consisting of immature and mature epithelial cells, reminiscent of intestine, with intervening mesenchymal-like septae (Figure 5c,

5g). Importantly, activin-treated cells gave rise to a heterogeneous teratoma-like cell mass with both mesodermal components as well as tubular structures of neural or epithelial origin (Figure 5d). Furthermore, follistatin-treated cells generated an encapsulated tissue with epithelial-like morphology, similar to control, and demonstrated cords of cells with intervening mesenchymal septae (Figure 5e). Both embryoid body and activin cases were not encapsulated and invaded into underlying tissue (data not shown).

Discussion

The induction of endoderm in vivo and in vitro is a complex and dynamic process. Therefore the generation of a simple ES cell culture system that could address fundamental questions, without the need for complex medium formulation or cell sorting is a major goal in the field. Our work demonstrates that an endoderm-like cell population can be induced by culture on fibronectin-coated collagen gel, without the use of activin, complex serum free medium, or serial cell sorting, which were previously thought to be essential for endoderm induction [15, 28]. We demonstrated that primitive epiblast and mesendoderm markers were transiently expressed in both control and follistatin cases (Figure 3). Since these cell populations are the direct precursors to endoderm, this suggests that definitive endoderm was induced by day 10 of culture on collagen gel. Activation of albumin (foregut), IFABP (midgut) and Cdx2 (hindgut) in subsequent late-stage differentiation (day 24) supports this assertion. In vivo differentiation of the day 10 endoderm-like cells with or without follistatin generated a homogenous population of epithelial cells, with intervening fibrous septae, suggesting that our endoderm-like cells remain committed. To our knowledge, this has yet to be reported in literature. Previously, renal capsule injection of endoderm-enriched populations resulted in heterogeneous groups of endoderm and mesoderm derivatives in mouse and human ES cell models of endoderm induction [28,60].

One of the surprising results in our studies is that activin, a known endoderm inducer, caused a decrease in endoderm specific gene and an 80% decrease in protein expression by day 10 of culture. Previous work demonstrated that activin-nodal-TGFβ signaling through Smad2/3 is essential for endoderm induction both in vivo and in vitro [15,28–30]. However, significant evidence suggests activin-nodal signaling might inhibit the early stages of ES cell differentiation in vitro [31,33,34]. Our results demonstrate that in vivo transplantation of activin-treated cells generate a heterogeneous teratoma-like mass with mesodermal, neural, and epithelial components (Figure 5d) suggesting that the activin-treated cells were still pluripotent. Gene expression kinetics data (Figure 3) show that day 10 activin-treated cells remain positive to major epiblast (Oct4, Fgf5 and Otx2) and mesendoderm markers (Brachyury, Goosecoid, Lhx 1) further strengthening the in vivo results. The activin-treated cells also demonstrated delayed hepatic gene and protein expression as shown in Figure 4. However, activin-treated cells were still competent to generate endoderm in vitro (Figure 4) and showed a remarkable proliferative potential in vivo (Figure 5b). Interestingly, the follistatin-treated population showed a 47% increase in the Foxa2-positive ES cell fraction by day 10, suggesting a role for endogenously secreted activin in ES cell self-renewal [33]. Alternatively, follistatin might interact with other pathways such as Wnt [61] and BMP [62] to induce differentiation. Further studies will be needed to determine the role of activin in ES cell differentiation using lineage tracing and proliferation studies.

To summarize, in this work we established a novel approach to induce a homogenous endoderm-like cell population that demonstrates lineage-appropriate gene and protein expression without resorting to cell sorting. Activin, normally an endoderm inducer, caused a dose-dependent decrease in endoderm induction, associated with an increase in its precursor epiblast population. One the other hand follistatin, a known activin inhibitor, increased the Foxa2 positive endoderm fraction to 78.4%. These studies demonstrate a novel technique to

induce the direct differentiation of endoderm from ES cells in vitro without resorting to cell sorting, and a new ability to induce critical, transient precursors which will assist in the development of ES-cell based cellular therapies.

Supplementary Material

Refer to Web version on PubMed Central for supplementary material.

Acknowledgments

NIH NRSA Fellowship

The authors thank Dr. Monica Casali, Dr. Halong Vu and Dr. Heidi Elmoazzen for experimental materials and advice. We also want to thank Dr. Kamran Badizadegan of the Massachusetts General Hospital Department of Pathology for histologic assessment of specimens and Robert Crowther for processing of tissue specimens. This work was supported by an NIH Biotechnology Fellowship as well as a National Research Service Award (NRSA).

References

1. Wells JM, Melton DA. Vertebrate endoderm development. Annu Rev Cell Dev Biol 1999;15:393–410. [PubMed: 10611967]
2. Oottamasathien S, Wang Y, Williams K, et al. Directed differentiation of embryonic stem cells into bladder tissue. Developmental biology. 2007
3. de Santa Barbara P, van den Brink GR, Roberts DJ. Molecular etiology of gut malformations and diseases. American journal of medical genetics 2002;115:221–230. [PubMed: 12503117]
4. Wobus AM, Boheler KR. Embryonic stem cells: prospects for developmental biology and cell therapy. Physiological reviews 2005;85:635–678. [PubMed: 15788707]
5. Poelmann RE. The head-process and the formation of the definitive endoderm in the mouse embryo. Anatomy and embryology 1981;162:41–49. [PubMed: 7283172]
6. Lawson KA, Pedersen RA. Cell fate, morphogenetic movement and population kinetics of embryonic endoderm at the time of germ layer formation in the mouse. Development (Cambridge, England) 1987;101:627–652.
7. Gardner RL, Rossant J. Investigation of the fate of 4–5 day post-coitum mouse inner cell mass cells by blastocyst injection. Journal of embryology and experimental morphology 1979;52:141–152. [PubMed: 521746]
8. Shivdasani RA. Molecular regulation of vertebrate early endoderm development. Developmental biology 2002;249:191–203. [PubMed: 12221001]
9. Gualdi R, Bossard P, Zheng M, et al. Hepatic specification of the gut endoderm in vitro: cell signaling and transcriptional control. Genes & development 1996;10:1670–1682. [PubMed: 8682297]
10. Sherwood RI, Jitianu C, Cleaver O, et al. Prospective isolation and global gene expression analysis of definitive and visceral endoderm. Developmental biology 2007;304:541–555. [PubMed: 17328885]
11. Tam PP, Behringer RR. Mouse gastrulation: the formation of a mammalian body plan. Mech Dev 1997;68:3–25. [PubMed: 9431800]
12. Ang SL, Wierda A, Wong D, et al. The formation and maintenance of the definitive endoderm lineage in the mouse: involvement of HNF3/forkhead proteins. Development 1993;119:1301–1315. [PubMed: 8306889]
13. Kanai-Azuma M, Kanai Y, Gad JM, et al. Depletion of definitive gut endoderm in Sox17-null mutant mice. Development 2002;129:2367–2379. [PubMed: 11973269]
14. Abe K, Niwa H, Iwase K, et al. Endoderm-specific gene expression in embryonic stem cells differentiated to embryoid bodies. Exp Cell Res 1996;229:27–34. [PubMed: 8940246]
15. Yasunaga M, Tada S, Torikai-Nishikawa S, et al. Induction and monitoring of definitive and visceral endoderm differentiation of mouse ES cells. Nat Biotechnol 2005;23:1542–1550. [PubMed: 16311587]

16. Zaret K. Developmental competence of the gut endoderm: genetic potentiation by GATA and HNF3/fork head proteins. Developmental biology 1999;209:1–10. [PubMed: 10208738]
17. Maguire T, Davidovich AE, Wallenstein EJ, et al. Control of hepatic differentiation via cellular aggregation in an alginate microenvironment. Biotechnology and bioengineering 2007;98:631–644. [PubMed: 17390383]
18. Sharma NS, Shikhanovich R, Schloss R, et al. Sodium butyrate-treated embryonic stem cells yield hepatocyte-like cells expressing a glycolytic phenotype. Biotechnology and bioengineering 2006;94:1053–1063. [PubMed: 16604521]
19. Novik EI, Maguire TJ, Orlova K, et al. Embryoid body-mediated differentiation of mouse embryonic stem cells along a hepatocyte lineage: insights from gene expression profiles. Tissue engineering 2006;12:1515–1525. [PubMed: 16846348]
20. Park J, Cho CH, Parashurama N, et al. Microfabrication-based modulation of embryonic stem cell differentiation. Lab on a chip 2007;7:1018–1028. [PubMed: 17653344]
21. Cho CH, Parashurama N, Park EY, et al. Homogeneous differentiation of hepatocyte-like cells from embryonic stem cells: applications for the treatment of liver failure. Faseb J. 2007
22. Zhou X, Sasaki H, Lowe L, et al. Nodal is a novel TGF-beta-like gene expressed in the mouse node during gastrulation. Nature 1993;361:543–547. [PubMed: 8429908]
23. Conlon FL, Lyons KM, Takaesu N, et al. A primary requirement for nodal in the formation and maintenance of the primitive streak in the mouse. Development (Cambridge, England) 1994;120:1919–1928.
24. Waldrip WR, Bikoff EK, Hoodless PA, et al. Smad2 signaling in extraembryonic tissues determines anterior-posterior polarity of the early mouse embryo. Cell 1998;92:797–808. [PubMed: 9529255]
25. Beppu H, Kawabata M, Hamamoto T, et al. BMP type II receptor is required for gastrulation and early development of mouse embryos. Developmental biology 2000;221:249–258. [PubMed: 10772805]
26. Winnier G, Blessing M, Labosky PA, et al. Bone morphogenetic protein-4 is required for mesoderm formation and patterning in the mouse. Genes & development 1995;9:2105–2116. [PubMed: 7657163]
27. Albano RM, Smith JC. Follistatin expression in ES and F9 cells and in preimplantation mouse embryos. The International journal of developmental biology 1994;38:543–547. [PubMed: 7848838]
28. Kubo A, Shinozaki K, Shannon JM, et al. Development of definitive endoderm from embryonic stem cells in culture. Development (Cambridge, England) 2004;131:1651–1662.
29. Chang H, Brown CW, Matzuk MM. Genetic analysis of the mammalian transforming growth factor-beta superfamily. Endocr Rev 2002;23:787–823. [PubMed: 12466190]
30. Okabayashi K, Asashima M. Tissue generation from amphibian animal caps. Current opinion in genetics & development 2003;13:502–507. [PubMed: 14550416]
31. Vallier L, Alexander M, Pedersen RA. Activin/Nodal and FGF pathways cooperate to maintain pluripotency of human embryonic stem cells. J Cell Sci 2005;118:4495–4509. [PubMed: 16179608]
32. James D, Levine AJ, Besser D, et al. TGFbeta/activin/nodal signaling is necessary for the maintenance of pluripotency in human embryonic stem cells. Development 2005;132:1273–1282. [PubMed: 15703277]
33. Beattie GM, Lopez AD, Bucay N, et al. Activin A maintains pluripotency of human embryonic stem cells in the absence of feeder layers. Stem Cells 2005;23:489–495. [PubMed: 15790770]
34. Ogawa K, Saito A, Matsui H, et al. Activin-Nodal signaling is involved in propagation of mouse embryonic stem cells. J Cell Sci 2007;120:55–65. [PubMed: 17182901]
35. Albano RM, Arkell R, Beddington RS, et al. Expression of inhibin subunits and follistatin during postimplantation mouse development: decidual expression of activin and expression of follistatin in primitive streak, somites and hindbrain. Development 1994;120:803–813. [PubMed: 7600958]
36. Rodgarkia-Dara C, Vejda S, Erlach N, et al. The activin axis in liver biology and disease. Mutat Res 2006;613:123–137. [PubMed: 16997617]
37. Miralles F, Czernichow P, Scharfmann R. Follistatin regulates the relative proportions of endocrine versus exocrine tissue during pancreatic development. Development 1998;125:1017–1024. [PubMed: 9463348]

38. Dunn JC, Yarmush ML, Koebe HG, et al. Hepatocyte function and extracellular matrix geometry: long-term culture in a sandwich configuration. Faseb J 1989;3:174–177. [PubMed: 2914628]
39. Livak KJ, Schmittgen TD. Analysis of relative gene expression data using real-time quantitative PCR and the 2(−Delta Delta C(T)) Method. Methods (San Diego, Calif 2001;25:402–408.
40. O'Brien LE, Zegers MM, Mostov KE. Opinion: Building epithelial architecture: insights from three-dimensional culture models. Nat Rev Mol Cell Biol 2002;3:531–537. [PubMed: 12094219]
41. Hisatomi Y, Okumura K, Nakamura K, et al. Flow cytometric isolation of endodermal progenitors from mouse salivary gland differentiate into hepatic and pancreatic lineages. Hepatology 2004;39:667–675. [PubMed: 14999685]
42. Notarianni E, Flechon J. Parietal endoderm cell line from a rat blastocyst. Placenta 2001;22:111–123. [PubMed: 11162360]
43. Tada S, Era T, Furusawa C, et al. Characterization of mesendoderm: a diverging point of the definitive endoderm and mesoderm in embryonic stem cell differentiation culture. Development 2005;132:4363–4374. [PubMed: 16141227]
44. Tang XB, Liu DP, Liang CC. Regulation of the transcription factor GATA-1 at the gene and protein level. Cell Mol Life Sci 2001;58:2008–2017. [PubMed: 11814053]
45. Schroeder TM, Jensen ED, Westendorf JJ. Runx2: a master organizer of gene transcription in developing and maturing osteoblasts. Birth Defects Res C Embryo Today 2005;75:213–225. [PubMed: 16187316]
46. Kim IM, Zhou Y, Ramakrishna S, et al. Functional characterization of evolutionarily conserved DNA regions in forkhead box f1 gene locus. The Journal of biological chemistry 2005;280:37908–37916. [PubMed: 16144835]
47. Britz O, Mattar P, Nguyen L, et al. A role for proneural genes in the maturation of cortical progenitor cells. Cereb Cortex 2006;16 (Suppl 1):i138–151. [PubMed: 16766700]
48. Ariizumi T, Asashima M. In vitro induction systems for analyses of amphibian organogenesis and body patterning. The International journal of developmental biology 2001;45:273–279. [PubMed: 11291857]
49. Pelton TA, Sharma S, Schulz TC, et al. Transient pluripotent cell populations during primitive ectoderm formation: correlation of in vivo and in vitro pluripotent cell development. Journal of cell science 2002;115:329–339. [PubMed: 11839785]
50. Burgess R, Cserjesi P, Ligon KL, et al. Paraxis: a basic helix-loop-helix protein expressed in paraxial mesoderm and developing somites. Developmental biology 1995;168:296–306. [PubMed: 7729571]
51. Merrill BJ, Pasolli HA, Polak L, et al. Tcf3: a transcriptional regulator of axis induction in the early embryo. Development (Cambridge, England) 2004;131:263–274.
52. Gotz M, Stoykova A, Gruss P. Pax6 controls radial glia differentiation in the cerebral cortex. Neuron 1998;21:1031–1044. [PubMed: 9856459]
53. Pelton TA, Bettess MD, Lake J, et al. Developmental complexity of early mammalian pluripotent cell populations in vivo and in vitro. Reprod Fertil Dev 1998;10:535–549. [PubMed: 10612459]
54. Ang SL, Jin O, Rhinn M, et al. A targeted mouse Otx2 mutation leads to severe defects in gastrulation and formation of axial mesoderm and to deletion of rostral brain. Development 1996;122:243–252. [PubMed: 8565836]
55. Fossat N, Chatelain G, Brun G, et al. Temporal and spatial delineation of mouse Otx2 functions by conditional self-knockout. EMBO reports 2006;7:824–830. [PubMed: 16845372]
56. Zaret KS. Liver specification and early morphogenesis. Mech Dev 2000;92:83–88. [PubMed: 10704889]
57. Zaret KS. Regulatory phases of early liver development: paradigms of organogenesis. Nat Rev Genet 2002;3:499–512. [PubMed: 12094228]
58. Wells JM, Melton DA. Early mouse endoderm is patterned by soluble factors from adjacent germ layers. Development 2000;127:1563–1572. [PubMed: 10725233]
59. Van Vranken BE, Romanska HM, Polak JM, et al. Coculture of embryonic stem cells with pulmonary mesenchyme: a microenvironment that promotes differentiation of pulmonary epithelium. Tissue engineering 2005;11:1177–1187. [PubMed: 16144454]

60. D'Amour KA, Agulnick AD, Eliazer S, et al. Efficient differentiation of human embryonic stem cells to definitive endoderm. Nature biotechnology 2005;23:1534–1541.

61. Willert J, Epping M, Pollack JR, et al. A transcriptional response to Wnt protein in human embryonic carcinoma cells. BMC Dev Biol 2002;2:8. [PubMed: 12095419]

62. Iemura S, Yamamoto TS, Takagi C, et al. Direct binding of follistatin to a complex of bone-morphogenetic protein and its receptor inhibits ventral and epidermal cell fates in early Xenopus embryo. Proc Natl Acad Sci U S A 1998;95:9337–9342. [PubMed: 9689081]

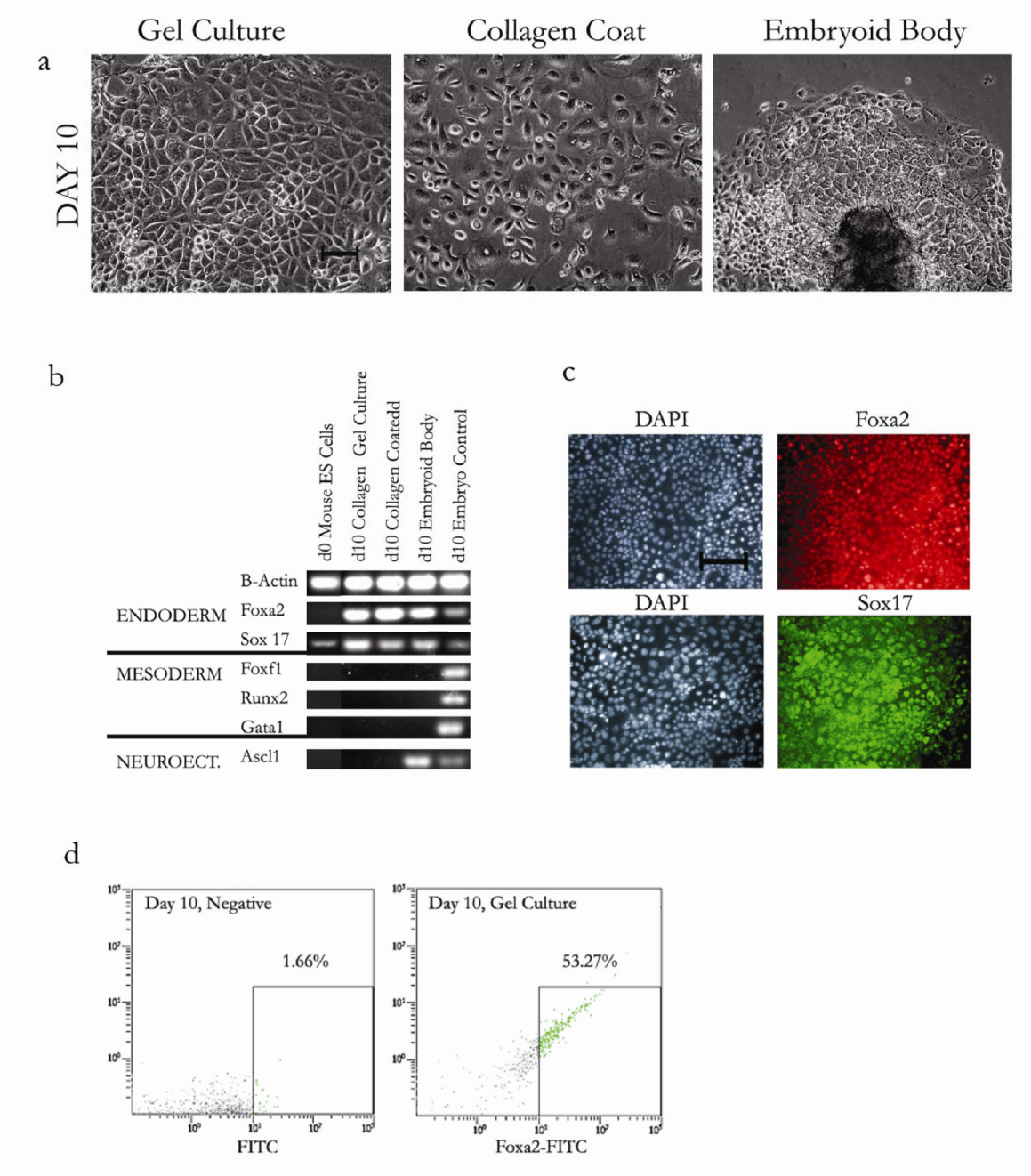

Figure 1.

Morphology, gene and protein expression of ES cells cultured on collagen gels. (a) Morphologic comparison of day 10 ES cells cultured on fibronectin-coated collagen gels (gel culture), tissue culture treated 12-well plate coated with collagen and fibronectin (collagen coat), and embryoid bodies plated on tissue culture plastic (embryoid bodies). Bar = 100 μm. (b) Germ layer specific gene expression measured by RT-PCR (30 cycles) of ES cells cultured on Day 10 in gel culture, collagen coat, and embryoid body configurations. Day 0 was used as a negative control and Day 10 mouse embryonic RNA was used as a positive control. Endoderm (Foxa2 and Sox 17), Mesoderm (Foxf1, Runx2, GATA1), and Neuroectoderm (Ascl1) were used to assess germ layers. (c) Immunoflourescence images of nuclear staining (DAPI) and

either Foxa2 (red), or Sox17 (green) staining of day 10 ES cells cultured on fibronectin-coated collagen gels (Gel Culture). Bar = 100 μm. (d) Flow cytometric analysis of Foxa2 positive cells of gel cultured ES cells on day 10. Positive fraction determined by threshold as shown.

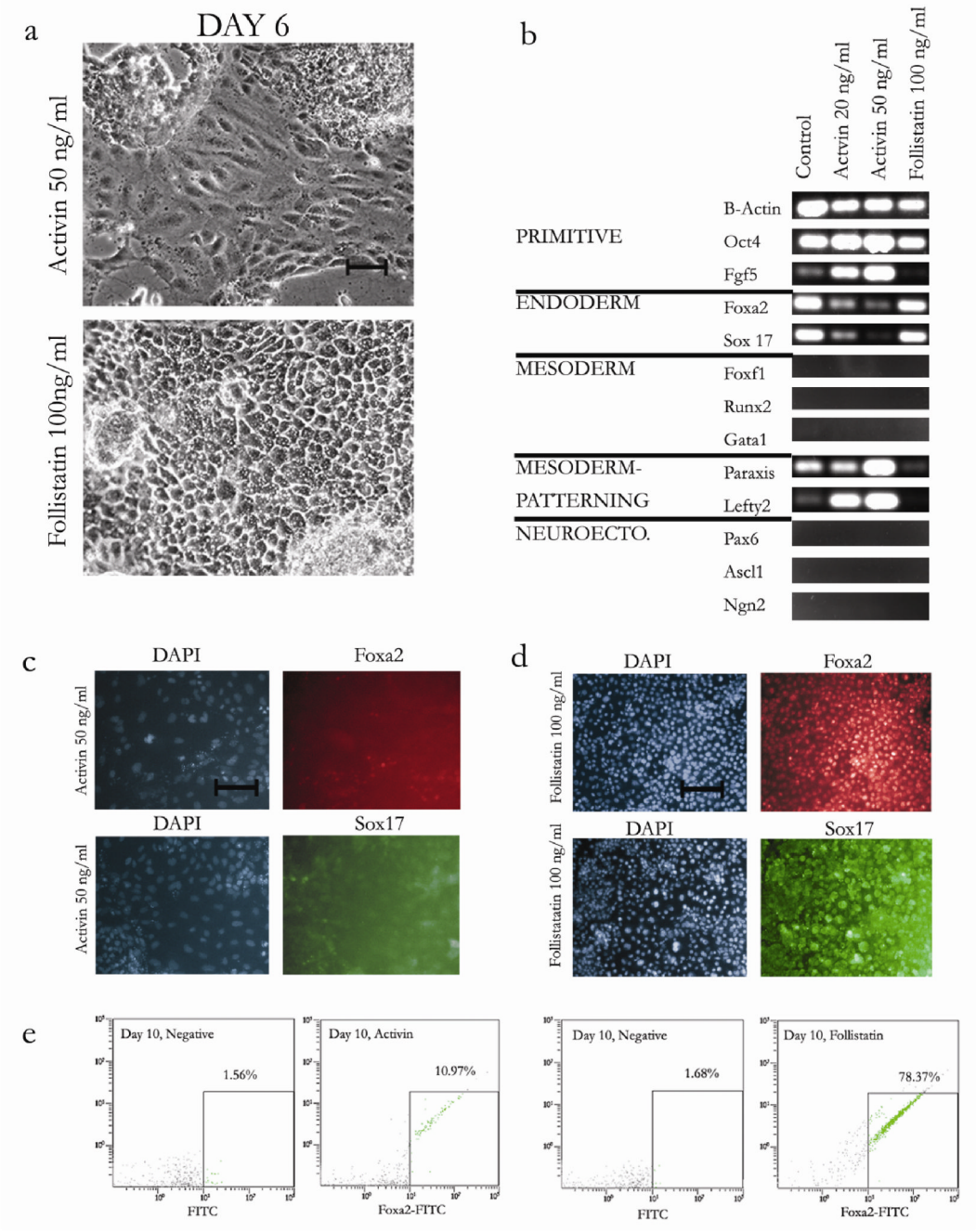

Figure 2.

Effects of activin and follistatin (activin inhibitor) on morphology, gene and protein expression of ES cells cultured on collagen gels. (a) Morphologic comparison of day 10 ES cells cultured in gel culture treated continuously with activin (20 ng/ml, 50 ng/ml) or follistatin (100 ng/ml). Bar = 100 μm. (b) Germ layer specific gene expression measured by RT-PCR (30 cycles, 5 ng RNA) of ES cells cultured on day 10 in gel culture. Primitive (Oct4, Fgf5), Endoderm (Foxa2 and Sox 17), Mesoderm (Foxf1, Runx2, GATA1), Early Mesoderm Patterning (Lefty2, Paraxis) and Neuroectoderm (Ascl1, Pax6, Ngn2) markers were used. (c,d) Immunoflourescence images of nuclear staining (DAPI) and either Foxa2 (red), or Sox17 (green), staining of day 10 embryonic stem cells cultured in gel culture, treated with activin

50 ng/ml or follistatin 100 ng/ml. Bar = 100μm. (e,f) Flow cytometric analysis of Foxa2 positive cells of gel cultured embryonic stem cells on day 10. Positive fraction determined by threshold as shown.

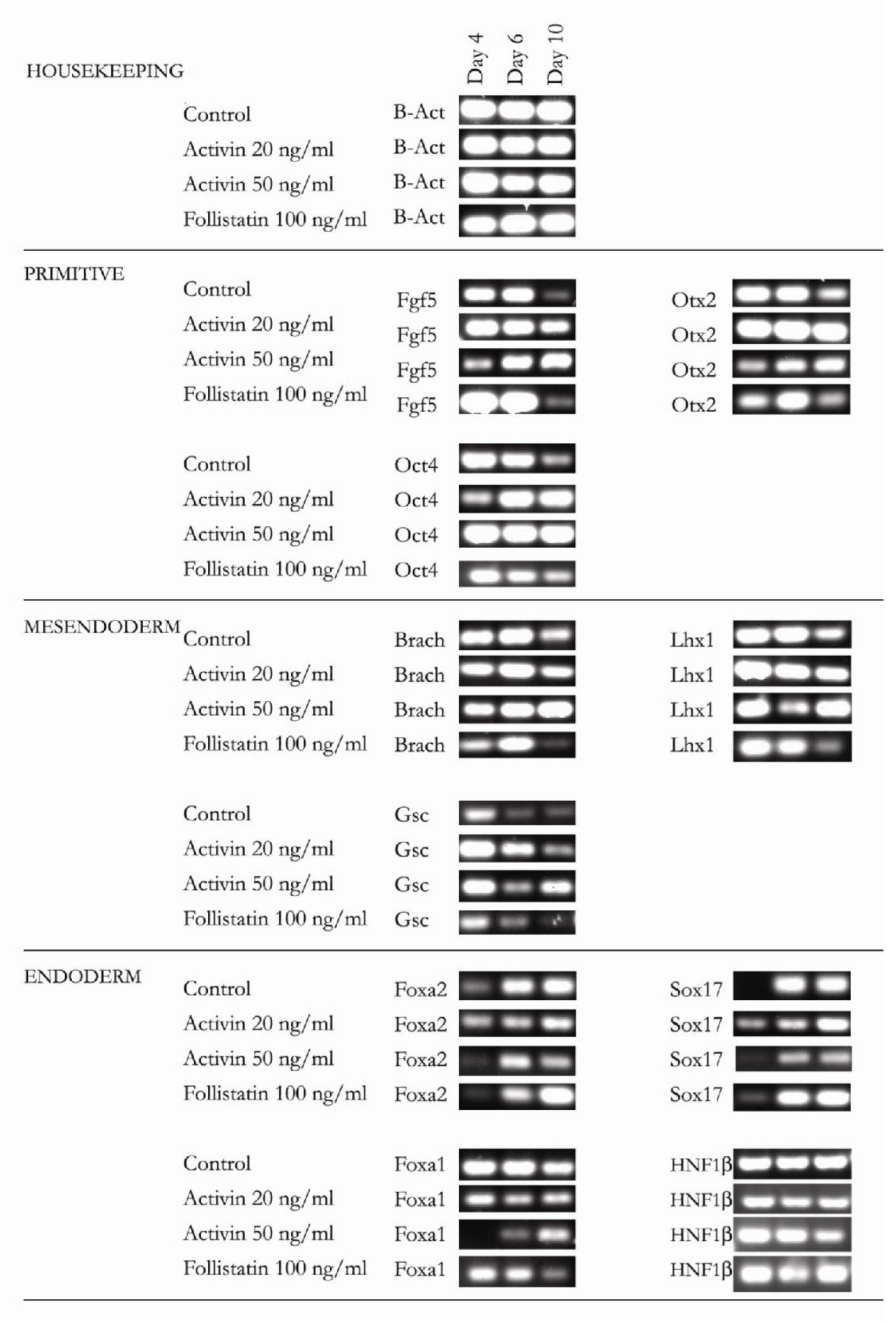

Figure 3.

Kinetics of epiblast, mesendoderm, and endoderm gene expression in control, activin and follistatin-treated cells. ES cells cultured in gel culture were treated with activin (20 ng/ml, 50ng/ml) and follistatin (100ng/ml). Markers for inner cell mass/epiblast (Oct4, Fgf5, Otx2), mesendoderm (Brachyury, Goosecoid, Lim 1 Homeobox) and endoderm (Foxa2, Sox 17, Foxa1, and HN1β) were used. Gene expression was measured by RT-PCR (30–35 cycles, 10 ng RNA) on days 4, 6, and 10.

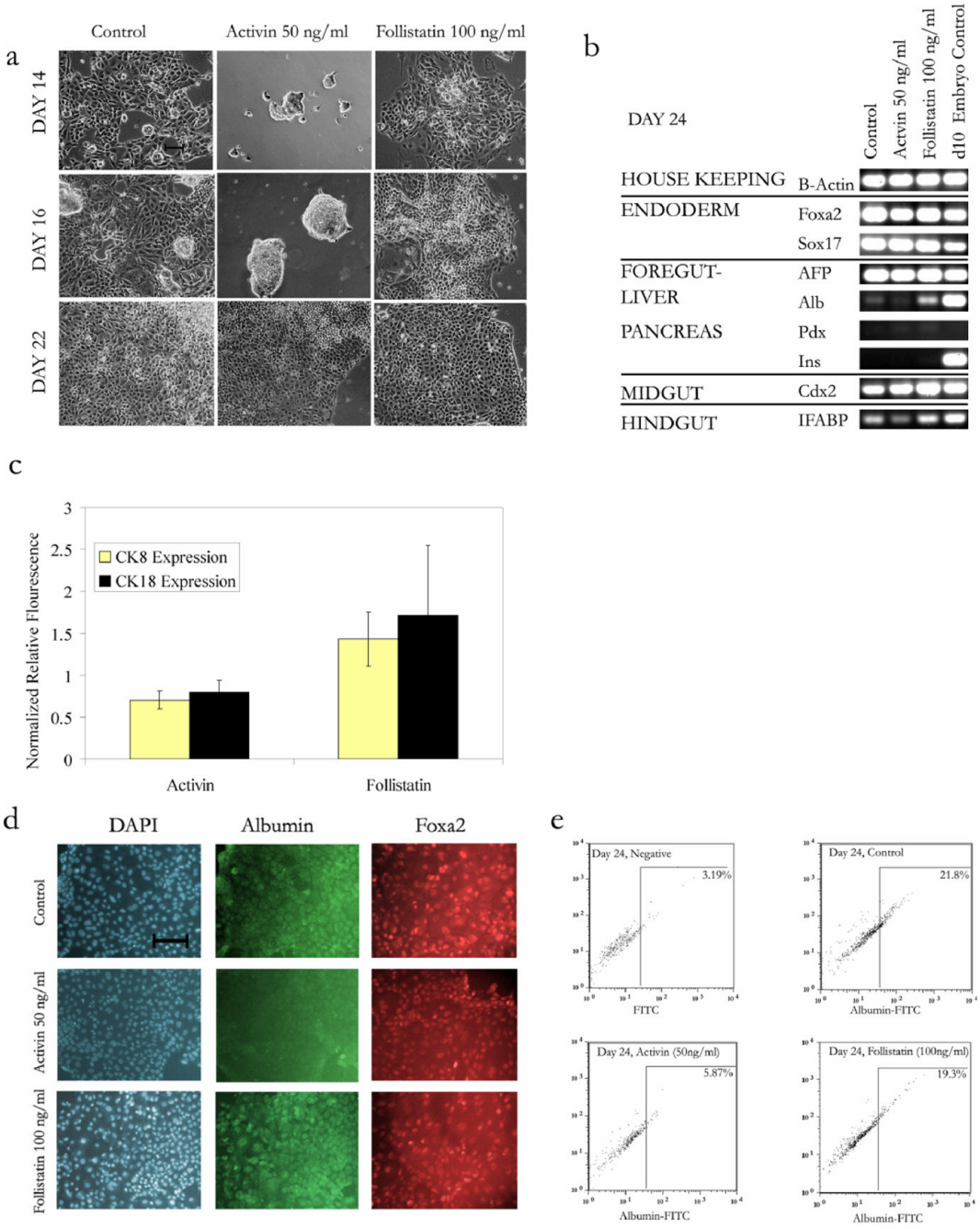

Figure 4.

Endoderm differentiation of control, activin, and follistatin-treated cells. (a) Morphologic comparison of day 10 control, activin or follistatin-treated embryonic stem cells re-cultured on fibronectin-coated collagen gels (Gel culture) in the presence of hepatic medium (C+H, see methods) with BMP2 (10 ng/ml), HGF (20 ng/ml) and Oncostatin 20 ng/ml). Bar = 100μm. (b) Gene expression was measured by RT-PCR (35 cycles, 10 ng RNA) for endoderm (Foxa2 and Sox17, foregut (AFP, Alb, Pdx1, Ins1), midgut (Cdx2), and hindgut (IFABP) markers. (c) Quantitative RT-PCR gene expression for two hepatic differentiation genes, CK 8 and CK 18. Data for activin and follistatin treated cells was normalized to control condition and is expressed as relative gene expression compared to control. (d) Immunoflourescence images (10×) of

nuclear staining (DAPI) and either Foxa2 (red), or albumin (green) staining of day 24 control, activin, or follistatin-treated cells re-cultured on fibronectin-coated collagen gels, in the presence of hepatic differentiation medium. (e) Flow cytometric analysis of albumin-positive cells differentiated in the presence of hepatic differentiation medium for control, activin, and follistatin. Positive fraction determined by threshold as shown.

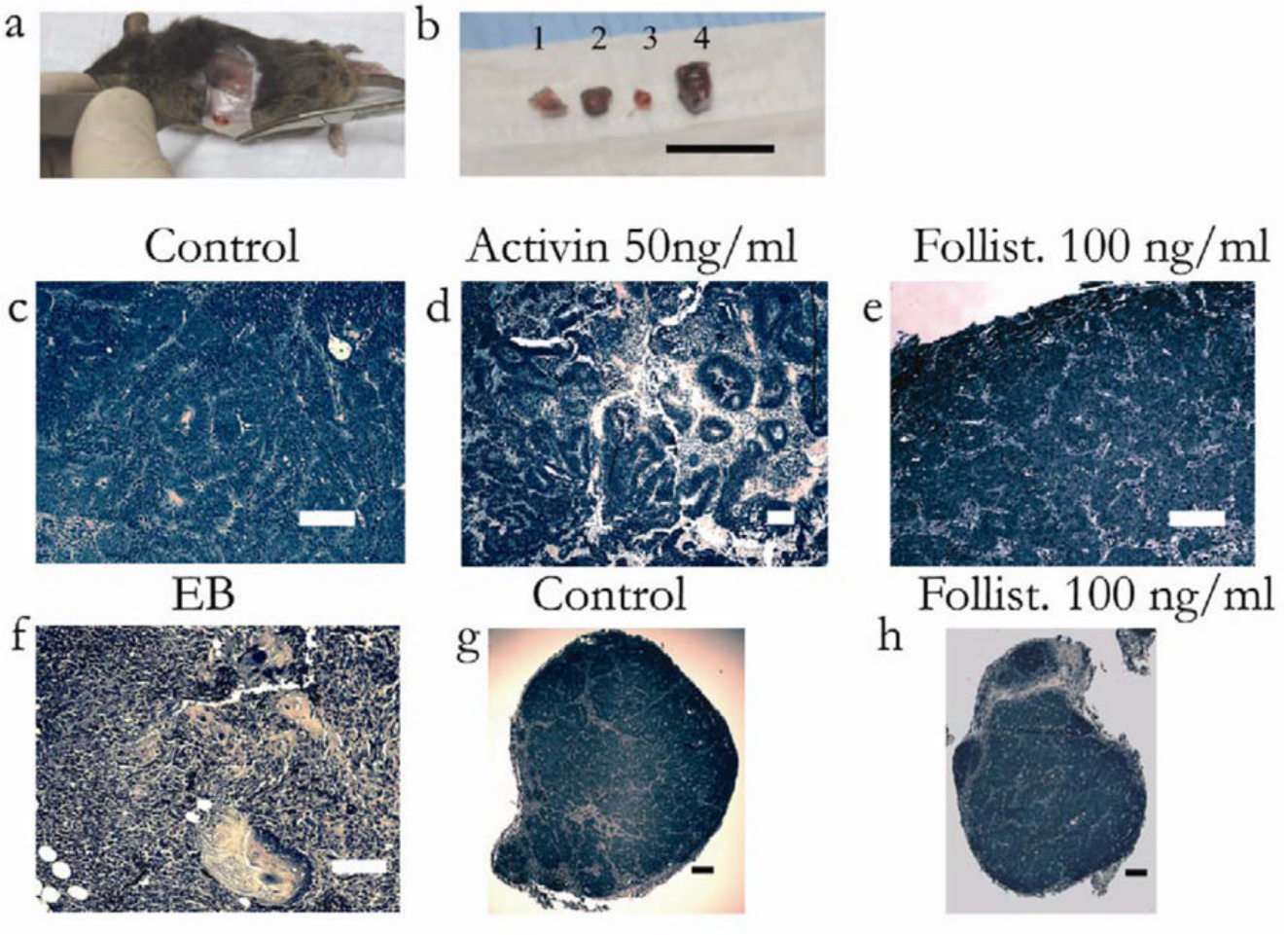

Figure 5.

In vivo differentiation of control, activin, and follistatin-treated cells. Day 10 gel cultured embryonic stem cells were mixed with NIH3T3 fibroblasts and subcutaneously implanted in syngeneic mice, for another 14 days. Conditions were, control (gel culture), activin (50ng/ml), and follistatin (100 ng/ml), and embryoid body control. (a) Encapsulated superficial mass demonstrated after incision. (b) Day 24 tissue masses after resection were embryoid body (1), gel culture (2), follistatin (100 ng/ml) (3), and activin (50 ng/ml) (4). Note that activin-treated cells resulted in the largest mass. Bar = 1 cm. H&E (Hematoxlin and Eosin) staining of implanted tissue masses. (c) Staining of gel culture demonstrates uniform epithelial-like cells with spindle-like septae. Bar = 100 μm. (d) Activin-treated cells, demonstrate heterogeneous, thick tubule-like structures, and mesenchymal elements. Bar = 100 μm. (e) Staining of follistatin-treated cells demonstrates uniform cords of epithelial cells separated by septae. Bar = 100 μm. (f) EB cells demonstrate heterogeneous tissue with skin, cartilage, and mesenchymal elements. Bar = 100 μm. (g) Low magnification image of the encapsulated gel culture mass. Bar = 200 μm. (h) Low magnification image of encapsulated follistatin-treated mass. Bar = 200 μm.

Table 1

Albumin positive fraction and mean intensity of albumin for day 24 cultured cells

Condition	% Positive	Mean Intensity
Negative Control (IgG)	3.19	13.7
Control (Activin 0ng/ml)	21.8	25.1
Activin 50ng/ml	5.87	15.8
Follistatin 100ng/ml	19.3	30.2